A quantum mechanics-based approach to model incident-induced dynamic driver behavior

Jiuh-Biing Sheu*

Institute of Traffic and Transportation, National Chiao Tung University, 4F, 114 Chung Hsiao W. Rd., Sec. 1, Taipei 10012, Taiwan ROC

Abstract

A better understanding of the psychological factors influencing drivers, and the resulting driving behavior responding to incident-induced lane traffic phenomena while passing by an incident site is vital to the improvement of road safety. This paper presents a microscopic driver behavior model to explain the dynamics of the instantaneous driver decision process under lane-blocking incidents on adjacent lanes. The proposed conceptual framework decomposes the corresponding driver decision process into three sequential phases: (1) initial stimulus, (2) glancing-around car-following, and (3) incident-induced driving behavior. The theorem of quantum mechanics in optical flows is applied in the first phase to explain the motion-related perceptual phenomena while vehicles approach the incident site in adjacent lanes, followed by the incorporation of the effect of quantum optical flows in modeling the induced glancing-around car-following behavior in the second phase. Then, an incident-induced driving behavior model is formulated to reproduce the dynamics of driver behavior conducted in the process of passing by an incident site in the adjacent lanes. Numerical results of model tests using video-based incident data indicate the validity of the proposed traffic behavior model in analyzing the incident-induced lane traffic phenomena. It is also expected that such a proposed quantum-mechanics based methodology can throw more light if applied to driver psychology and response in anomalous traffic environments in order to improve road safety.

1. Introduction

Incident-induced lane traffic phenomena and their impacts on road safety remain critical in traffic management and control. According to previous literature [30,31,28,29], the complexity and difficulty in characterizing incident-induced lane traffic phenomena may stem from the incident-induced mandatory lane traffic maneuvers from blocked lanes to adjacent lanes, and the resulting approaching delays of traffic moving in the adjacent lanes upstream to the incident site. On the other hand, the aforementioned anomalous traffic phenomena caused by incidents are time-varying, and may vary with incident characteristics, such as incident location and duration, and the instantaneous traffic flow conditions. Hall [13] further claimed that the severity of incident-induced

delay might rely mainly on three factors, such as the nature of incidents, roadway conditions, and execution of incident clearance. Particularly, the resulting delay may increase unusually as the traffic flow adjusting to the roadway capacity does not have alternatives for traffic diversion. For these reasons, modeling of incident-induced lane traffic maneuvers is a critical step for addressing non-recurrent traffic congestion problems.

Although recent years have seen an increasing interest in research in analyzing incident effects on traffic flows, most of the existing approaches appeared to be macroscopic traffic modeling, where traffic is treated as a dynamic flow state, and limited to freeway incident cases. The well-known kinematic wave (KW) theory was used by Messer et al. [20] to predict link travel time in the presence of freeway incidents, followed by the studies of Newell [24,23] which aimed to characterize the phenomena of traffic flows queuing at freeway bottlenecks using a simplified version of KW

---

* Tel.: +886 2 2349 4963; fax: +886 2 2349 4953.
  E-mail address: jbsheu@mail.nctu.edu.tw.

theory. Similarly, the fundamentals of the KW theory were used by Daganzo et al. [10] to model the phenomena of moving bottlenecks on freeways, where the slow vehicles found in traffic streams were treated discretely as moving boundaries affecting the corresponding traffic streams. Despite the potential advantages of these pioneering KW-based theories in analyzing queuing propagation of traffic streams and the resulting delays at the bottlenecks of freeways, the preset fundamental diagrams, i.e., the relationships among flow, density, and speed, from which most of these models stem may not hold in incident cases. This argument appears plausible particularly when the effects of incident-induced lane-changing maneuvers from blocked lanes to adjacent lanes are noticeable. More specifically, the existing KW-based analytical models may not be reliable in characterizing the effects of drivers' rubbernecking behavior in adjacent lanes, which may also contribute significantly to the travel delays of vehicles passing by an incident site.

In contrast to the aforementioned macroscopic traffic flow theories, microscopic models attempt to formulate laws reproducing the behavior of individual vehicles by integrating certain human factors, and classical physics/mechanics theories (e.g., Newton theorems). That is, in the microscopic traffic domain, researchers tend to treat each vehicle as a unit particle with respective moving behavior so as to infer the macroscopic traffic flow phenomena through aggregating the dynamic operational features of these "traffic particles". For instance, there are a variety of car-following models [16,14,6, 8,32] that can be found in previous literature, where the basis of car-following theories is rooted in the manner with which a following vehicle responds to the corresponding vehicle ahead via instantaneous speed adjustment for safety concerns, as depicted in [6]. Therein, factors such as the reaction time, inter-vehicle spacing, and the relative speed observed between a pair of the given vehicles following and ahead are incorporated into model formulation.

Nevertheless, the lack of a deep insight in the variations of psychological factors under anomalous traffic environments, e.g., lane-blocking incidents, and their influences in driver behavior may contribute to the existing car-following models falling short in deducing the resulting lane traffic phenomena. For instance, under heavily congested conditions, some drivers may take risks to adopt dangerously short clearances to prevent vehicles in the adjacent lanes from entering the gap immediately in front of their vehicles [26]. In addition, some other factors such as drivers' rubbernecking and driving under pressure while passing by an incident site may also cause these rational microscopic traffic behavior models to be invalid for incident cases [14]. Furthermore, there is a consensus in the area of traffic engineering that a traffic system is composed of three types of elements: (1) road users, (2) vehicles, (3) infrastructure, thus contributing to diverse traffic phenomena. Unfortunately, most of traffic phenomena can hardly be characterized by theories of pure physics and mechanics due to the involvement of human factors, external environments, and the intricate inter-effects among these elements varying with time and space. Thus, despite a variety of macroscopic

and microscopic traffic models published, it is necessary to develop respective models for different study purposes. Particularly, the microscopic traffic behavior modeling should no longer be limited to the characterization of specific "traffic-particle" locomotion using classical physical theorems; rather, such human psychological and physiological factors as the perceptions of moving environments and the induced responses should be conceptualized to reproduce "real" driver behavior.

Due to the above reasons, we aim to propose a specific microscopic traffic behavior model to characterize the dynamics of individual driver behavior of the adjacent lane in the process of passing by an incident site. Considering the potential effects of drivers' psychological factors in influencing the corresponding driving behavior, the proposed model incorporates several factors, including the stimulus oriented from the variations of optic flows, curiosity, and internal pressure into the model formulation. Herein, a quantum mechanical approach is utilized to characterize the initial stimulus oriented from the variations of optical flows, and the resulting driving response, termed glancing-around car-following behavior, followed by the formulation of respective rubbernecking car-following and lane-changing maneuvers to reproduce the potential driving behavior of the given adjacent-lane vehicle conducted to pass by the incident site. In this study, we tend to adopt the claims of computational judgment theories [3,2,11,18,7,1] instead of the ecological optic theories [12,17] to deal with the procedure of transmitting the driver's perceived motion-related phenomena and the induced driving responses. As noted in [1], relative to the ecological optic approaches which postulate that information can be directly available from a user's optic array and immediately usable without further transformation process, the computational judgment theories posit that complicated mental calculations can be needed to process the visual stimuli of moving images into behavioral outcomes. Therein, the judgment errors may occur in the perception of moving images due to a wave-image duality in transferring visual information, and thus an uncertainty relationship between the perception of speed and the focal point of version may inherently exist in any observation. For these reasons, the quantum mechanics of optic flow is utilized to characterize such dynamic and uncertain properties of the driver's perception of moving environments under the condition of approaching an incident site in this study. The entire operational phases of the proposed model are detailed in the following section.

In addition, it is worth mentioning that the proposed model aims to reproduce the dynamics of incident-induced individual driver behavior utilizing the theories of quantum optic flow. The model itself and the incorporation of the effect of quantum optical flows in modeling incident-induced microscopic traffic behavior cannot be found in any previous literature. Therein, we attempt to show the high potential of the study in bridging areas among applied physics, traffic engineering, and applied psychology. This may also help clarify the unique contribution of the paper to related areas.
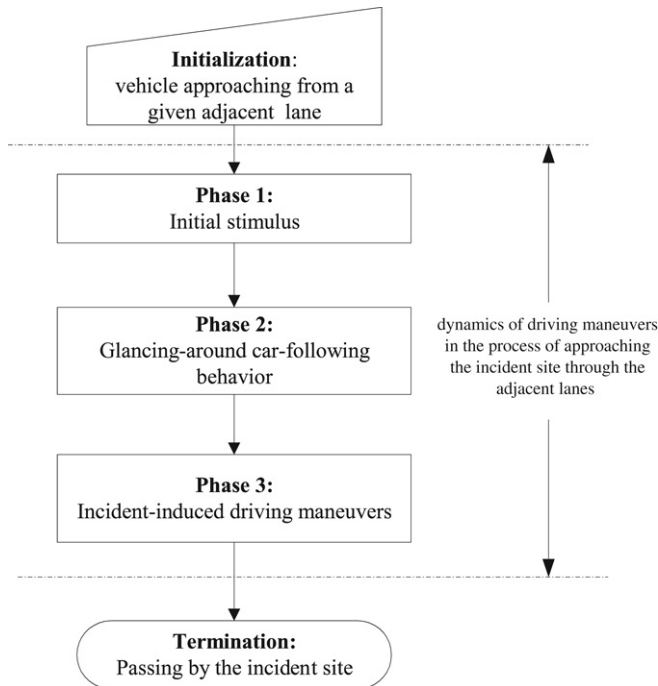
Fig. 1. Conceptual framework of the proposed microscopic model.

2. Modeling

The proposed incident-induced driver behavior model mainly consists of three sequential phases: (1) initial stimulus, (2) glancing-around car-following, and (3) incident-induced driving behavior, to characterize the sequence of drivers' potential behavior responding to the incident effect as they approach an incident site from the corresponding adjacent lanes. Fig. 1 illustrates the proposed conceptual framework. The corresponding hypothesis is postulated below.

Now, let us consider a case of an approaching vehicle, which moves in the corresponding adjacent lane upstream from the incident site without the acquisition of the instantaneous incident information. Given that in the aforementioned vehicular approaching process, the target driver may perceive the anomalous changes in section-wide traffic flows at a given location x and given time t due to the instantaneous variation of the optical flow within the visual scope, contributing to the instantaneous stimulus in the psychological domain, followed by an intuitive speed adjustment maneuver. In the classical optic flow field, such visual stimuli of moving images are physically conceptualized with the changing patterns of light incidence on a projection surface (termed the trajectories on the retina) to intercept the time-varying optic array [17]. Alternatively, we tend to conceptualize the aforementioned optical flow-induced stimulus-response process in the quantum optic field, followed by a psychophysical momentum function to infer the driver's post-stimulus response, i.e., the instantaneous speed adjustment, as depicted in phase 1 (termed as initial stimulus) of the proposed model. Then, the target driver may be spontaneously distracted by the instantaneous traffic phenomena, and try to find out where the source is from,

resulting in the glancing-around car-following behavior which is reproduced in the second phase. In reality, such an effect may not be durable, and in the proposed model, it is assumed that the corresponding duration may vary with drivers, and end up with the time when the incident site is recognized by the target driver. Then, it is followed by the third phase, which reproduces the incident-induced driving decision process in which the target driver may decide: either to conduct the maneuver of car following with more watchfulness, or change to farther lanes until the incident site has been passed.

Compared to the existing microscopic models, three unique features are exhibited in the proposed model. First, adopting the ideas of Baker [1], we regard the aforementioned initial stimulus as resulting from the sharp change in a human's optical flows when the target driver perceives the anomalous variations in section-wide traffic flow conditions. Therein, the optic array is assumed to be a quantum state, and thus the stimulus in the optic field by light can be transmitted using the fundamentals of quantum mechanics. Second, following the generation of the initial stimulus, the resulting curiosity may further drive the target driver to find out the sources causing the instantaneous traffic phenomena, thus forming the so-called glancing-around effect that is assumed to have a certain influence on the instantaneous car-following behavior of the target driver. Accordingly, a respective glancing-around car-following model is proposed to reproduce the resulting driver behavior in the second phase. Third, we claim that after the recognition of the incident site, the driving behavior of the target driver can be influenced to a certain extent by the incident event, and such an effect may vary with the relative distance between the target vehicle and the incident site. Therefore, the incident effect is incorporated in formulating the incident-induced driving decision making process, which is detailed in the third phase.

Based on the above postulations, the respective traffic behavior models formulated in the aforementioned three phases are introduced in the following.

Phase 1: Initial stimulus

The purpose of this phase is to build a dynamic optical flow model employing a quantum mechanical approach that can be used to derive the dynamic relationship between the stimulus and response of the target driver oriented from the perception of sudden changes of vehicular movements approaching an incident site. The quantum mechanics-based optical flow model can be regarded as an extension of a cognitive approach [18, 7] which is also an alternative way applied to characterizing the impact of optical flow on individual behavior, relative to the ecological optic theories [12,17]. Here, we borrow the conclusions of Baker [1], and apply quantum mechanics to develop the incident-induced optical flow model. The developmental process is presented as follows.

First, let us consider the initial condition that a vehicle (termed the target vehicle i) moves on a given lane l without knowing the occurrence of an incident downstream on the adjacent lane l'. According to the theories of quantum
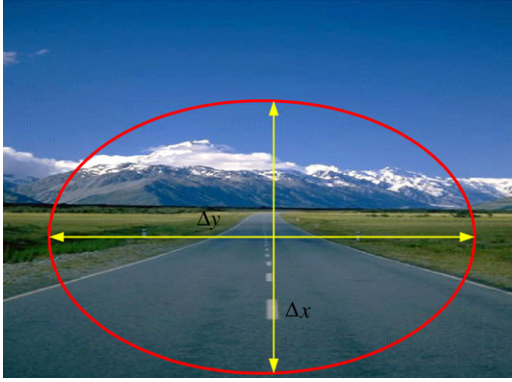
Fig. 2. Definition of a peripheral visual field.

optical flow [22,25,4,15],we can define a peripheral visual field ($F[\Delta x(t), \Delta y(t)]$), as shown in Fig. 2, to describe the probability-related assignment of attention spreading across the longitudinal (x) and lateral (y) dimensions of the field, given by

$$(\Delta x(t))(v_i(t)) = A_x, \quad \forall t \tag{1}$$

$$(\Delta y(t))(v_i(t)) = A_y, \quad \forall t \tag{2}$$

where $\Delta x(t)$ and $\Delta y(t)$ refer to the instantaneous visual scope in the x- and y- dimensions of the visual field at time t, respectively; $v_i(t)$ represents the instantaneous speed of the target vehicle i at time t; A_x and A_y are two constants associated with the x- and y-dimensions. Here, the scope of the peripheral visual field may change with the instantaneous speed ($v_i(t)$). As claimed in [1], a higher vehicular speed may require the concentration of processing resources, thus forming the driver's "tunnel version", which is a manifestation of forward focused motion. Therefore, a trade-off relationship between $\Delta y(t)$ and $v_i(t)$ may exist as presented in Eq. (2); and similar deduction also applies to the relationship between $\Delta x(t)$ and $v_i(t)$ as shown in Eq. (1).

Now, suppose that in the process of approaching the unperceived incident site, the driver of the target vehicle i, moving with an instantaneous speed $v_i(t)$, perceives the sudden changes of section-wide traffic flows composed of a certain number of vehicles ahead (denoted by J_F) within the corresponding visual field ($F[\Delta x(t), \Delta y(t)]$) at time t. Accordingly, we can obtain the instantaneous psychophysical momentum oriented from each given perceived vehicle j_F ($M_{j_F}(t)$) and the corresponding psychophysical energy function ($E_{j_F}(t)$) by

$$M_{j_F}(t) = m_{j_F} \times [\Delta v_{j_F \to i}(t)] \times U_i(t) \tag{3}$$

$$E_{j_F}(t) = \frac{m_{j_F} \times [\Delta v_{j_F \to i}(t)]^2 \times U_i(t)}{2} \tag{4}$$

where j_F represents a given vehicle perceived by the target driver within the instantaneous visual field $F[\Delta x(t), \Delta y(t)]$ at time t; m_{j_F} represents the perceived light mass associated with j_F; $\Delta v_{j_F \to i}(t)$ represents the perceived instantaneous speed of j_F relative to the target vehicle i at time t; $U_i(t)$ refers to the instantaneous degree of watchfulness associated with the target driver i in driving safely at time t, indicating that a driver with a higher level of $U_i(t)$ may perceive a greater

psychophysical momentum.[1] However, according to Baker [1], the psychophysical energy should be defined as a function of the frequency of the optical flow, considering the stability for the quantum solution. Thus, employing the classical quantum equations, the following conditions should also hold for each vehicle j_F perceived within the visual field.

$$M_{j_F}(t) = \frac{h}{\lambda_{j_F}(t)} \tag{5}$$

$$E_{j_F}(t) = h \times f_{j_F}(t) \tag{6}$$

where $\lambda_{j_F}(t)$ and $f_{j_F}(t)$ represent the wavelength and frequency associated with the quantum optical flow oriented from a given vehicle j_F perceived by the target driver at time t and h refers to an action constant. Correspondingly, the perceived image associated with j_F can be characterized in a waveform with the respective wavelength ($\lambda_{j_F}(t)$) and frequency ($f_{j_F}(t)$) given by

$$\lambda_{j_F}(t) = \frac{h}{M_{j_F}(t)} \tag{7}$$

$$f_{j_F}(t) = \frac{E_{j_F}(t)}{h}. \tag{8}$$

Using Eqs. (3), (4), (7) and (8), together with the fundamentals of wave packet formation, we can obtain the aggregate wavelength ($\lambda_{J_F}(t)$) of the wave packet resulting from the sudden changes of section-wide traffic flows (J_F) perceived within the binocular vision field, and according to the early literature [5,21,1], the resulting wave packet spreading ($\Delta x(\tilde{t})$) can be derived as

$$\Delta x(\tilde{t}) = \frac{\lambda_{J_F}(t)}{2}. \tag{9}$$

Here, $\Delta x(\tilde{t})$, similar to the definition of $\Delta x(t)$, can be regarded as the "post-stimulus" visual scope in the x-dimension of the visual field immediately after the moment of initial stimulus at time $\tilde{t}$, where $\tilde{t} \approx t$. According to Eq. (1), we can then derive $v_i(\tilde{t})$, which refers to the instantaneous speed adjusted by the target vehicle i intuitively responding to the perceived sudden changes in the quantum optical flows, and is also the output from this phase.

Phase 2: Glancing-around car-following behavior

This phase describes a respective dynamic driver behavior model to reproduce the potential glancing-around driving behavior of the target vehicle i following the phase of initial stimulus. The proposed glancing-around car-following model is derived mainly based on the postulation that due to personal curiosity about the instantaneous traffic phenomena the target

---

[1] In the proposed model, both the psychophysical momentum ($M_F(t)$) of optical flow and that of the corresponding psychophysical energy ($E_F(t)$) can be regarded as the intermediums to motivate the target driver's further response to the source of stimulus (i.e., the sudden changes of lane traffic flows), and thus, they may lie commonly on the instantaneous watchfulness ($U_i(t)$) of the target driver i in driving safety at time t. This is one of our main reasons for incorporating the driver's watchfulness factor into the above model formulation.

vehicle may remain running in the same lane, but adjust its speed based on the perceived vehicles (J_F), including the vehicle just ahead ($i - 1$), dispersing across multiple lanes in the forward direction within the instantaneous visual field ($F[\Delta x(\tilde{t}), \Delta y(\tilde{t})]$). Such a curiosity-driven driving maneuver may remain until the incident event is perceived by the target driver.

The theories of quantum optical flow are used in this phase [5,21]. As mentioned previously, a driver's attention dispersal in the instantaneous visual field $F[\Delta x(\tilde{t}), \Delta y(\tilde{t})]$ can be characterized in a probability distribution form, where there would be the highest probability for locating the focal point at the center of the visual field. Here, we propose the use of a two-dimensional Gaussian wave packet ($G_{F[\Delta x(\tilde{t}), \Delta y(\tilde{t})]}[x(\tilde{t}), y(\tilde{t})]$) to estimate the joint probability associated with each perceived vehicle spreading across the x- and y-dimensions of the visual field $F[\Delta x(\tilde{t}), \Delta y(\tilde{t})]$. Then, the resulting glancing-around car-following behavior of the target driver is treated as the outcome of the target vehicle's speed adjustment for continuously responding to the aggregate quantum optical flow resulting from the perceived vehicles dispersing ahead. Accordingly, a unique glancing-around car-following model is proposed as

$$
\begin{aligned}
\dot{v}_i(\tilde{t}) &= \alpha_1 \times \sum_{\forall j_F \in J_F} w_{i,j_F}(\tilde{t}) \times M_{j_F}(\tilde{t}) \\
&= \alpha_1 \times U_i(\tilde{t}) \times \sum_{\forall j_F \in J_F} w_{i,j_F}(\tilde{t}) \\
&\quad \times \left\{ m_{j_F} \times [\Delta v_{j_F \to i}(\tilde{t})] \right\}
\end{aligned}
\tag{10}
$$

where $\dot{v}_i(\tilde{t})$ refers to the resulting speed adjustment conducted by the target vehicle i at time $\tilde{t}$; α_1 represents a preset parameter; $w_{i,j_F}(\tilde{t})$ represents a time-varying weighting value indicating the relative magnitude of the target driver's attention assigned at a given perceived vehicle j_F at time $\tilde{t}$; $M_{j_F}(\tilde{t})$, as defined in Eq. (3), refers to the instantaneous psychophysical momentum oriented from a given perceived vehicle j_F measured at time $\tilde{t}$. Here, $w_{i,j_F}(\tilde{t})$ can be further expressed as

$$
w_{i,j_F}(\tilde{t}) = \frac{G_{F[\Delta x(\tilde{t}), \Delta y(\tilde{t})]}[x_{j_F}(\tilde{t}), y_{j_F}(\tilde{t})]}{\sum\limits_{\forall j'_F \in J_F} G_{F[\Delta x(\tilde{t}), \Delta y(\tilde{t})]}[x_{j'_F}(\tilde{t}), y_{j'_F}(\tilde{t})]}
\tag{11}
$$

where $G_{F[\Delta x(\tilde{t}), \Delta y(\tilde{t})]}[x_{j_F}(\tilde{t}), y_{j_F}(\tilde{t})]$ represents the joint probability obtained from the instantaneous two-dimensional Gaussian wave packet ($G_{F[\Delta x(\tilde{t}), \Delta y(\tilde{t})]}[x(\tilde{t}), y(\tilde{t})]$) with respect to the location ($[x_{j_F}(\tilde{t}), y_{j_F}(\tilde{t})]$) of a given perceived vehicle j_F in the x- and y-dimensions of the target driver's visual field $F[\Delta x(\tilde{t}), \Delta y(\tilde{t})]$; a similar definition also applies to $G_{F[\Delta x(\tilde{t}), \Delta y(\tilde{t})]}[x_{j'_F}(\tilde{t}), y_{j'_F}(\tilde{t})]$ in which j'_F refers to any vehicle perceived by the target driver at time $\tilde{t}$. Here, $G_{F[\Delta x(\tilde{t}), \Delta y(\tilde{t})]}[x(\tilde{t}), y(\tilde{t})]$ has the following generalized form:

$$
G_{F[\Delta x(\tilde{t}), \Delta y(\tilde{t})]}[x(\tilde{t}), y(\tilde{t})] = \frac{e^{-\frac{1}{2}\left[\frac{[x(\tilde{t}) - \mu_{F_x}(\tilde{t})]^2}{\sigma_{F_x}^2(\tilde{t})} + \frac{[y(\tilde{t}) - \mu_{F_y}(\tilde{t})]^2}{\sigma_{F_y}^2(\tilde{t})}\right]}}{2\pi \times \sigma_{F_x}(\tilde{t}) \times \sigma_{F_y}(\tilde{t})}.
\tag{12}
$$

In Eq. (12), $\mu_{F_x}(\tilde{t})$ and $\mu_{F_y}(\tilde{t})$ represent the centers of the instantaneous wave packet in the x- and y- dimensions, respectively; $\sigma_{F_x}(\tilde{t})$ and $\sigma_{F_y}(\tilde{t})$ refer to the spatial spreads of the instantaneous wave packet along x- and y-dimensions.

The rationale of the proposed glancing-around car-following model mentioned above is discussed below in several aspects. First, according to the previous literature [30,29], in the presence of a lane-blocking incident, any given vehicle approaching the incident site may adjust its speed based not only on the front vehicle but also on the perceived group, which is also approaching the incident. Such an argument, in reality, relies on the hypothesis that under conditions of lane-blocking incidents, any given vehicle tends to coordinate its speed with an aggregate speed of the incident-impacted traffic flows moving ahead in response to incident effects on section-wide traffic flows. Accordingly, it is inferred that the instantaneous multi-vehicle momentum perceived by the target driver should be incorporated in the proposed model to characterize the aforementioned effect. Second, from a psychological point of view, it seems agreeable that the magnitude of speed adjustment of the target vehicle appears to be dependent on the watchfulness ($U_i(\tilde{t})$) of the corresponding target driver given the instantaneous section-wide traffic flow conditions. Empirically, a driver with more caution appears more sensitive to the changes of optical flows, thus contributing to a greater degree of speed reduction upon perceiving an unexpected reduction in the aggregate speed of the downstream section-wide traffic flows. In contrast, a careless driver may exhibit a relatively insensitive attitude given the same traffic flow conditions. Therefore, the factor of $U_i(\tilde{t})$ is proportional to the speed adjustment, as can be seen in Eq. (10). Third, both the perceived aggregate vehicular momentum (i.e., the sum in terms of $M_{j_F}(\tilde{t})$ shown in Eq. (10)) and the resulting speed adjustment ($\dot{v}_i(\tilde{t})$) are of directional correlation. For instance, given that only one front vehicle j_F is perceived by the target driver i at time $\tilde{t}$ and the perceived relative speed ($\Delta v_{j_F \to i}(\tilde{t})$) is negative representing a backward relative speed perceived by i, it may result in a negative speed adjustment, i.e., deceleration ($\dot{v}_i(\tilde{t}) < 0$), of the target vehicle i, according to Eq. (10), in response to the perceived vehicular momentum moving backward to the target driver. Similarly, if the perceived relative speed $\Delta v_{j_F \to i}(\tilde{t})$ is positive, the resulting speed adjustment of the target vehicle i may turn out to be positive, i.e., acceleration ($\dot{v}_i(\tilde{t}) > 0$) according to the proposed glancing-around car-following model.

Phase 3: Incident-induced driving behavior

The driving behavior model proposed in this phase serves mainly to reproduce the dynamics of the potential driving behavior conducted by the target driver in the process of passing by the incident site after recognizing the existence of an incident. Unlike the previous phase of glancing-around car-following behavior which is oriented from the target driver's curiosity about the anomalous changes in section-wide traffic flow conditions before recognizing the incident ahead, this phase aims to characterize the potential driving behavior of

the target driver after perceiving the existence of the incident. Herein, two primary incident-induced driving behaviors are considered, including (1) rubbernecking-driven car-following and (2) lane-changing, which are viewed as the two potential primary driving behavior conducted by the target driver in this phase when passing by the incident site. They are detailed in the following.

The incident-induced rubbernecking-driven car-following behavior depicted here stems from the target driver's diversion partly from the perceived traffic flows spreading toward the incident site, coupled with the personal driving pressure which may amplify upon approaching the incident site from the adjacent lane. Such mixed psychological factors thus contribute to the incident-induced rubbernecking-driven car-following behavior.

To characterize the aforementioned driving behavior, we propose a specific incident-induced rubbernecking car-following model, which is extended from the aforementioned glancing-around car-following model, but has the following distinctive features relative to the existing car-following models. First, it is assumed that the instantaneous speed adjustment ($\dot{v}_i(t')$) of the target vehicle i may depend not only on the perceived front vehicle's maneuvers but also on the degree of personal diversion on the perceived incident event as well as the affected vehicles present upstream from the incident site in the blocked lanes. In reality, our postulation proposed here mainly considers the phenomenon that under such conditions of incidents, any given target vehicle may tend to adjust itself to the incident effects on multi-lane traffic flows (i.e., the traffic flows on both the blocked lane and the adjacent lanes), and thus coordinating its speed not only with the time-varying safety spacing relative to the corresponding front vehicle but also with the potential lane changes from the blocked lane. Particularly, the corresponding mandatory lane-changing effect from the blocked lane may become increasingly significant while the target vehicle is approaching the incident-site. Supporting arguments can also be found in the previous literature [30,31,29]. Accordingly, an incident-induced rubbernecking-driven car-following model is proposed as

$$\dot{v}_i(t') = \alpha_2 \times w_{i,i-1}(t') \times M_{i-1}(t') - \alpha_3 \times w_{i,\Lambda}(t')$$

$$\times \left\{ E_\Lambda(t') + \left[\sum_{\forall j_\Lambda} E_{j_\Lambda}(t') \right] \times \bar{p}_{\Lambda \to i} \right\} \quad (13)$$

where $\dot{v}_i(t')$ refers to the resulting speed adjustment conducted by the target driver i at time t'; α_2 and α_3 are two positive parameters; $M_{i-1}(t')$ represents the instantaneous psychophysical momentum associated with the front vehicle $i-1$ perceived by the target driver at time t'; $E_\Lambda(t')$ and $E_{j_F}(t')$ represent the psychophysical energy functions associated with the given incident Λ and a given vehicle j_Λ present in the blocked lane upstream from the incident site Λ perceived by the target driver at time t'; $\bar{p}_{\Lambda \to i}$ refers to the lane-changing possibility, anticipated by the target driver, from the blocked lane upstream from the incident site Λ to the target lane where the target vehicle i is present; $w_{i,i-1}(t')$ and $w_{i,\Lambda}(t')$

represent time-varying weighting values indicating the relative magnitude of the target driver's attention assigned at the perceived front vehicle $i-1$ and the incident site Λ at time $\tilde{t}$, respectively. Similar to the formulation defined in Eq. (11) and (12), here, $w_{i,i-1}(t')$ and $w_{i,\Lambda}(t')$ can be further expressed by

$$w_{i,i-1}(t')$$
$$= \frac{G_{F[\Delta x(t'),\Delta y(t')]}[x_{i-1}(t'), y_{i-1}(t')]}{G_{F[\Delta x(t'),\Delta y(t')]}[x_{i-1}(t'), y_{i-1}(t')] + G_{F[\Delta x(t'),\Delta y(t')]}[x_\Lambda(t'), y_\Lambda(t')]} \quad (14)$$

$$w_{i,\Lambda}(t')$$
$$= \frac{G_{F[\Delta x(t'),\Delta y(t')]}[x_\Lambda(t'), y_\Lambda(t')]}{G_{F[\Delta x(t'),\Delta y(t')]}[x_{i-1}(t'), y_{i-1}(t')] + G_{F[\Delta x(t'),\Delta y(t')]}[x_\Lambda(t'), y_\Lambda(t')]}$$
$$= 1 - w_{i,i-1}(t'). \quad (15)$$

As can be seen in Eq. (13), the instantaneous speed adjustment of the target vehicle i involves two major terms: one dependent on the perception of the target driver in terms of the instantaneous psychophysical momentum ($M_{i-1}(t')$) associated with the front vehicle $i-1$, and the other resulting from the incident effect coupled with the anticipation of the target driver in the potential disturbance of the vehicular lane changes from the blocked lane to the corresponding adjacent lane, thus represented by the corresponding psychophysical energy diversion (i.e., $E_\Lambda(t') + [\sum_{\forall j_\Lambda} E_{j_\Lambda}(t')] \times \bar{p}_{\Lambda,i}(t')$). In addition, considering the trade-off effect in terms of the attention magnitude with respect to the perceived front vehicle and the incident-induced lane traffic phenomena in the blocked lane, the associated time-varying weights $w_{i,i-1}(t')$ and $w_{i,\Lambda}(t')$ are involved in Eq. (13). Correspondingly, the farther the target vehicle i is from the incident site, the more the speed adjustment of the target vehicle i, depending on the driving behavior of the perceived front vehicle. In contrast, the closer the target vehicle approaches to the incident site, the more the speed adjustment of the target vehicle that may be influenced by the perception of the incident event and the induced anticipation of lane-changing disturbance from the blocked lane. Such anticipated incident-induced effects oriented from the blocked lane may turn out to be increasingly significant as the target vehicle approaches the incident site until fully passed by the incident.

In addition, it is noteworthy that since the instantaneous psychophysical momentum ($M_{i-1}(t')$) shown Eq. (13) is directional, it can contribute to the corresponding speed adjustment of the target driver (positive or negative), depending on the perceived relative speed ($\Delta v_{i-1 \to i}(\tilde{t})$). In contrast, the second term of Eq. (13) is not a directional quantity, thus, contributing to a purely negative effect in speed adjustment in the equation. Accordingly, two extreme cases are discussed below to illustrate the applicability of the proposed model for incident cases, relatively to traditional car-following theories.

In the first case, let us consider a simple condition where there is no affected vehicle present in the blocked lane upstream from the incident site as the target vehicle is approaching via the adjacent lane. Under the aforementioned condition, the speed

adjustment estimation shown in Eq. (13) may turn out to be

$$\dot{v}_i(t') = \alpha_2 \times w_{i,i-1}(t') \times M_{i-1}(t') - \alpha_3 \times E_\Lambda(t')$$
$$= \alpha_2 \times [1 - w_{i,\Lambda}(t')]$$
$$\times \left\{ m_{i-1} \times [\Delta v_{i-1 \to i}(t')] \times U_i(t') \right\}$$
$$- \alpha_3 E_\Lambda(t'). \qquad (16)$$

Herein, it is inferred that given no affected vehicles perceived in the blocked lane, the speed adjustment of the target driver may be influenced not only by the relative speed of the front vehicle $i - 1$ but also by the relative magnitude of perception with respect to the incident event nearby, according to the proposed model, due to the driver's curiosity mixed with the watchfulness over the perceived incident event. Such an inference may not be coherent with the results reproduced by any of the existing car-following models, but appears to be more suitable for characterizing the real driving behavior of the target driver under the condition of driving by a bottleneck, e.g., an incident. Furthermore, according to the tradeoff relationship between the instantaneous visual scope (Δy) in the lateral dimension and moving speed (see Eq. (2)), while Δy increases, the instantaneous speed of the target vehicle must be decreased to pay more attention on the perceived incident event nearby. Again, this is why we claim the applicability of the proposed model for the characterization of incident-induced driving behavior, relative to the existing car-following theories.

The second case illustrates another phenomenon supposing that only a certain number of vehicles present in the blocked lane upstream to the incident site are perceived (i.e., no front vehicle is perceived within the visual scope). Then, the proposed incident-induced speed adjustment model Eq. (13) can be simplified as

$$\dot{v}_i(t') = -\alpha_3 \times \left\{ E_\Lambda(t') + \left[\sum_{\forall j_\Lambda} E_{j_\Lambda}(t') \right] \times \bar{p}_{\Lambda,i} \right\}. \qquad (17)$$

In reality, Eq. (17) indicates that even if there is no front vehicle present, the target driver may still decelerate, rather than drive at will, while approaching the incident site due to the mixed psychological factors mentioned above. Such inference may further apply to a similar case, which supposes that no vehicles are perceived within the visual scope of the target driver, and then the speed adjustment of the target vehicle i can be induced by

$$\dot{v}_i(t') = -\alpha_3 \times E_\Lambda(t'). \qquad (18)$$

That is, the target vehicle may decelerate to respond to the incident effect on the driver's attention within the corresponding visual scope.

The following model depicts a lane-changing decision process of the target driver to be further away from the blocked lane while approaching to the perceived incident event. Herein, we propose two sequential stages, including (1) pre-action decision-making and (2) in-action lane-changing operation, involved in the corresponding decision process to reproduce the incident-induced lane-changing behavior of the target driver. The details on these two stages are described below.

The model proposed for the pre-action decision-making stage serves to determine whether an action of incident-induced lane changing is needed at any given time t' in this phase (i.e., Phase 3). If yes, the following in-action lane-changing operational stage is triggered; otherwise, the aforementioned incident-induced rubbernecking-driven car-following behavior will still be conducted by the target driver. Here, we propose that the driver's pre-action decision process for further lane changing can be mainly influenced by three key factors: (1) the anticipated lane-changing effect from the blocked lane, (2) the perceived lane-changing status in the target lane (i.e., the lane that the target vehicle is present in), and (3) the relative group-based speeds in the adjacent lanes in comparison with that in the target lane. The corresponding rationales are provided in the following.

As such, the judgment driven by the anticipated lane-changing effect from the blocked lane stems from the safety concern of the target driver to avoid the potential lane-changing disturbance from the blocked lane, and thus, the proposed decision rule is given by

$$\text{IF} \quad E_\Lambda(t') + \left[\sum_{\forall j_\Lambda} E_{j_\Lambda}(t') \right] \times \bar{p}_{\Lambda,i}(t') \overset{\geq}{\underset{<}{}} \delta_i^1(t'),$$

$$\text{THEN lane changing} \begin{matrix} \text{is} \\ \text{is not} \end{matrix} \text{considered} \qquad (19)$$

where $\delta_i^1(t')$ represents a time-varying threshold referring to the upper bound associated with the target driver i with respect to the tolerance of the corresponding anticipated lane-changing disturbance from the blocked lane at time t'. In practice, $\delta_i^1(t')$ is also a psychological factor, which is correlated with the driver's instantaneous attitude, emotionally and sensibly, toward the lane-changing interruption from the blocked lane, represented by $E_\Lambda(t') + [\sum_{\forall j_\Lambda} E_{j_\Lambda}(t')] \times \bar{p}_{\Lambda,i}(t')$, thus contributing to Eq. (19), which is used to determine if an incident-induced lane-changing maneuver is expected by the target driver at time t'.

The judgment with respect to the perceived lane-changing status of the target lane relies on the magnitude of the perceived instantaneous energy function ($\sum_{\forall j_{\ell_i \to \ell}} E_{j_i \ell \to \ell}(t')$) associated with the lane-changing movements from the present target lane (ℓ_i) to the corresponding adjacent lane (ℓ), which is farther away from the blocked lane (ℓ_Λ), as illustrated in Fig. 3. Accordingly, we have the following decision rule:

$$\text{IF} \quad \sum_{\forall j_{\ell_i \to \ell}} E_{j_{\ell_i \to \ell}}(t') \overset{\geq}{\underset{<}{}} \delta_i^2(t'),$$

$$\text{THEN lane changing} \begin{matrix} \text{is} \\ \text{is not} \end{matrix} \text{considered} \qquad (20)$$

where $\delta_i^2(t')$ represents a time-varying threshold with respect to the acceptability of the target driver i to follow the lane-changing behavior moving from lane ℓ_i to lane ℓ at time t'. According to this decision rule, this psychological factor, the target driver may attempt to conduct lane-changing maneuvers when the perceived lane-changing-out energy function ($\sum_{\forall j_{\ell_i \to \ell}} E_{j_{\ell_i \to \ell}}(t')$) is greater or

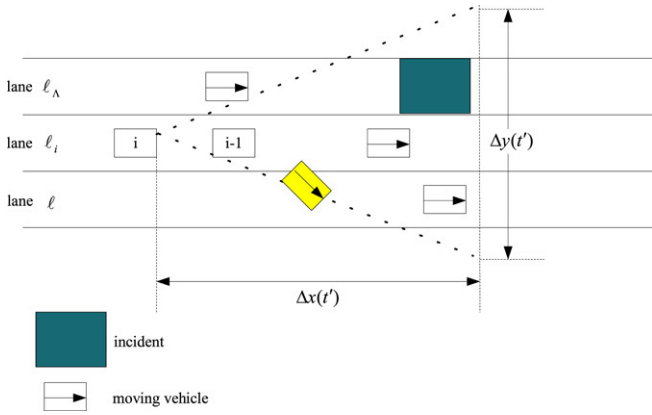Fig. 3. Illustration of the perceived lane changes to the adjacent lane ℓ.

Fig. 4. Illustration of the turning angle restriction.

equal to the corresponding threshold $\delta_i^2(t')$; otherwise, the incident-induced rubbernecking-driven car-following behavior mentioned previously may remain conducted by the target vehicle i until passed by the incident site.

In addition to the perceived lane-changing status in and out of the target lane (ℓ_i), the relative group-based speed in the corresponding adjacent lane (ℓ) is also a significant factor influencing this stage for the determination of lane-changing behavior. Utilizing the aforementioned concept of the instantaneous visual scope ($F[\Delta x(t'), \Delta y(t')]$), the target driver i may compare the relative aggregate group speed in the corresponding adjacent lane ℓ with the instantaneous speed of the front vehicle ($i - 1$) perceived in the target lane ℓ_i. Once the front group speed in the adjacent lane ℓ perceived within the instantaneous visual scope ($F[\Delta x(t'), \Delta y(t')]$) is greater than the instantaneous speed of the front vehicle ($i - 1$), the target vehicle may consider lane-changing. Correspondingly, if the following condition holds, the target driver may attempt to conduct lane-changing maneuvers.

$$\text{IF} \quad \frac{\sum_{j_\ell=1}^{N_\ell(t')} v_{j_\ell}(t')}{N_\ell(t')} - v_{i-1}(t') \geqslant \delta_i^3(t'),$$

THEN lane changing is considered (21)

where $v_{j_\ell}(t')$ represents the instantaneous speed of a given vehicle (j_ℓ) involved in the vehicular group of the corresponding adjacent lane ℓ perceived at time t'; $N_\ell(t')$ represents the number of vehicles involved in the perceived group of the corresponding adjacent lane ℓ at time t'. Similarly, $\delta_i^3(t')$ refers to a time-varying threshold in terms of the acceptability of the target driver i to conduct the lane-changing behavior moving from lane ℓ_i to lane ℓ based on the perceived group speed of lane ℓ relative to the instantaneous speed of the vehicle moving ahead at time t'.

Given that the target driver i triggers the pre-action lane-changing process at time t', and completes the corresponding judgment at time t'' the following in-action lane-changing stage may trigger at time t'' if one of the aforementioned three conditions holds. Herein, the in-action lane-changing rules are proposed to characterize the decision logic rules of the target driver i to complete the lane-changing maneuvers.
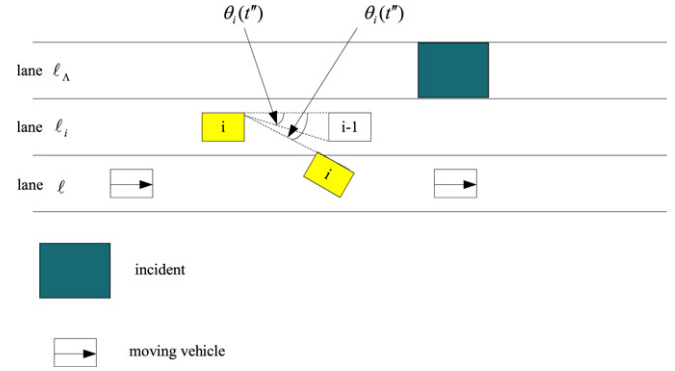
Compared to the aforementioned pre-action decision, which aims to determine whether or not the incident-induced lane-changing maneuvers are necessary, the target driver's decision made in this stage may aim to conduct the lane-changing maneuver safely and smoothly in response to the diversity of traffic conditions in both the target and adjacent lanes. To characterize such an in-action driving decision process, we herein propose four decision rules: two necessary conditions associated with the intra-lane traffic influence factors, whereas the others are associated with the inter-lane traffic influence factors, to determine if the incident-induced lane-changing maneuver can be completed successfully by the target driver in the in-action lane-changing phase. That is, the incident-induced lane-changing behavior can be safely implemented only when all the following four required conditions are satisfied.

- Condition 1: Restriction of turning angle of the target vehicle i ($\theta_i(t'')$).

This condition takes account of the potential conflict points that may exist between the target vehicle (i) and the front vehicle ($i - 1$) in the target vehicle's lane changing process, as shown in Fig. 4. To implement the lane-changing behavior, the following condition must hold.

$$\theta_i(t'') \geqslant \theta_{i-1}(t'') \tag{22}$$

where $\theta_i(t'')$ refers to the anticipated turning angle of the target driver i at the onset of conducting the lane-changing behavior; $\theta_{i-1}(t'')$ represents a parameter in terms of the instantaneous conflict angle of the front vehicle $i - 1$ perceived by the target driver i at time t'', and is given by

$$\theta_{i-1}(t'') = \tan^{-1} \left\{ \frac{W_{i-1}}{x_i(t'') - x_{i-1}(t'') - L_{i-1} - X_i^{\text{safe}}} \right\} \tag{23}$$

where $x_i(t'')$ and $x_{i-1}(t'')$ represent the instantaneous locations of the vehicular heads associated with the target vehicle i and the front vehicle $i - 1$ relative to the incident site in the longitudinal dimension at time t'', respectively; L_{i-1} and W_{i-1} represent the physical length and width of the front vehicle $i - 1$, respectively; X_i^{safe} is the static minimum safety spacing between the target and front vehicles.

- Condition 2: Restriction of latitudinal spacing between the target (i) and front ($i - 1$) vehicles of the original target lane.

$$\Phi_i^{\sin\theta_i}(t'' + \Delta t_i) = \frac{3[\vec{v}_i^{\cos}(t'')]^2 + 8\dot{v}_i(t'')S_i(t'') - 2[\vec{v}_i^{\cos}(t'')] \times \eta(t'') + 2[\vec{v}_i^{\sin}(t'')] \times \{\eta(t'') - [\vec{v}_i^{\cos}(t'')]\}}{2\dot{v}_i(t'')}$$

$$\tilde{W}_{i-1}(t'' + \Delta t_i) = W_{i-1} \times [1 + \alpha_4 \times v_{i-1}(t'' + \Delta t_i)]$$

$$\Delta t_i = \frac{\eta(t'') - 2\vec{v}_i^{\cos}(t'')}{2\dot{v}_i(t'')}$$

Box I.

Given $\theta_i(t'')$, the following condition should also hold in order to avoid the collision of the target vehicle (i) with the front vehicle of the original target lane (ℓ_i) in the process of lane changing.

$$\Phi_i^{\sin(\theta_i)}(t'' + \Delta t_i) \geqslant \tilde{W}_{i-1}(t'' + \Delta t_i) \tag{24}$$

where $\Phi_i^{\sin(\theta_i)}(t'' + \Delta t_i)$ refers to the moving distance of the target vehicle i in the latitudinal direction in the process of lane changing at time $t'' + \Delta t_i$; $\tilde{W}_{i-1}(t'' + \Delta t_i)$ is the dynamic vehicular width[2] of the front vehicle ($i-1$) in the original target lane (ℓ_i) perceived by the target vehicle i at time $t'' + \Delta t_i$; Δt_i represents the time spent by the target vehicle i moving with a maximum safety distance in the longitudinal direction in the process of lane changing to avoid the collision with the front vehicle ($i-1$). Theoretically, $\Phi_i^{\sin(\theta_i)}(t''+\Delta t_i)$, $\tilde{W}_{i-1}(t''+\Delta t_i)$, and Δt_i shown above are the functions of the microscopic characteristics of the target and the front vehicles in the original target lane, and can be derived, respectively, as given in Box I; where $\dot{v}_i(t'')$ represents the instantaneous speed adjustment conducted by the target vehicle i at time t'' in the process of lane changing; α_4 is a pre-set parameter; $\vec{v}_i^{\cos}(t'')$ represents the relative speed of the target vehicle i in comparison with the vehicle ahead $i-1$ in the longitudinal direction at time t'' in the process of lane changing; and similarly, $\vec{v}_i^{\sin}(t'')$ represents that it is in the latitudinal direction; $S_i(t'')$ corresponds to the relative moving distance that is allowed to be conducted by the target vehicle i along the longitudinal direction in the process of lane changing, in consideration of the avoidance of the collision with the front vehicle ($i-1$) of the original target lane (ℓ_i) at time t''; $\eta_i(t'')$ is merely a dummy variable which can be replaced by $\sqrt{4[\vec{v}_i^{\cos}(t'')]^2 + 8\dot{v}_i(t'')S_i(t'')}$. Here, $\vec{v}_i^{\cos}(t'')$, $\vec{v}_i^{\sin}(t'')$, and $S_i(t'')$ can be further expressed as

$$\vec{v}_i^{\cos}(t'') = v_i(t'') \times \cos[\theta_i(t'')] - v_{i-1}(t'') \tag{25}$$

$$\vec{v}_i^{\sin}(t'') = v_i(t'') \times \sin[\theta_i(t'')] \tag{26}$$

$$S_i(t'') = x_i(t'') - x_{i-1}(t'') - L_{i-1} - X_i^{\text{safe}}. \tag{27}$$

Note that, conveniently, the instantaneous speed of the front vehicle $i-1$ is herein assumed to be constant in the process of the lane-changing maneuver conducted by the target vehicle i.

---

[2] The concept of the dynamic vehicular length and width is proposed in the previous literature [9] to characterize the dynamic safety spacing of between any given pair of two adjoining vehicles moving in roundabouts [9], and here, we apply the concept of the dynamic vehicular width to formulate $\tilde{W}_{i-1}(t'' + \Delta t_i)$ used to characterize the latitudinal safety spacing between the target vehicle i and the front vehicle $i-1$ in the original target lane (ℓ_i) in the process of lane changing.

- Condition 3: Restriction of the dynamic safety spacing between the target vehicle i and the rear vehicle $j_\ell + 1$ in the corresponding adjacent lane (ℓ) that is aimed by the target vehicle to move via the lane-changing behavior.

This condition is rooted in our speculation in terms of the target driver's safety concerns to avoid the potential collision with the rear vehicle ($j_\ell + 1$) of the adjacent lane (ℓ). It is worth mentioning that in the lane-changing process, the target driver may be concerned about the ability of the corresponding rear vehicle ($j_\ell + 1$) in responding to such an instantaneous inter-lane traffic interruption relative to incident-free conditions. In addition, it is commonly agreed that the corresponding rear driver's behavior to respond to the lane-changing phenomena present ahead may not be the same as conducted in normal car-following cases.

To mimic the aforementioned psychological conditions of the target driver, first, we introduce the concept of a conflict point ($X_{j_\ell+1 \to i}^c(t'' + \Delta t_i)$), as

$$X_{j_\ell+1 \to i}^c(t'' + \Delta t_i) = x_i(t'' + \Delta t_i) + L_i + X_i^{\text{safe}}. \tag{28}$$

Utilizing the notation of $X_{j_\ell+1 \to i}^c(t'' + \Delta t_i)$ defined above, we speculate that under lane-blocking incident conditions, any potential incident-induced lane traffic phenomena, e.g., lane changes and queue overflows may occur ahead such that both the target vehicle (i) and the rear vehicle ($j_\ell + 1$) can be forced to brake anytime and anywhere. Therefore, the target driver i may need to judge if the dynamic safety spacing between the post-action location ($x_{j_\ell+1}(t'' + \Delta t_i)$) of the rear vehicle $j_\ell + 1$ and the conflict point $X_{j_\ell+1 \to i}^c(t'' + \Delta t_i)$ is greater than zero. Correspondingly, the lane-changing maneuver conducted by the target driver i should follow the condition shown in Eq. (29) to ensure driving safety after completing the lane-changing behavior.

$$x_{j_\ell+1}(t'' + \Delta t_i) - X_{j_\ell+1 \to i}^c(t'' + \Delta t_i) \geqslant 0$$

$$\Rightarrow x_{j_\ell+1}(t'') - \left\{ v_{j_\ell+1}(t'') \times \tau_{j_\ell+1} - \frac{[v_{j_\ell+1}(t'')]^2}{2\bar{d}_{j_\ell+1}} \right\}$$

$$- \left\{ x_i(t'') + \frac{[v_i(t'') \times \cos[\theta_i(t'')]]^2}{2\bar{d}_i} + L_i + X_i^{\text{safe}} \right\} \geqslant 0$$

$$\Rightarrow x_{j_\ell+1}(t'') - x_i(t'')$$

$$\geqslant \left\{ v_{j_\ell+1}(t'') \times \tau_{j_\ell+1} - \frac{[v_{j_\ell+1}(t'')]^2}{2\bar{d}_{j_\ell+1}} \right\}$$

$$+ \frac{[v_i(t'') \times \cos[\theta_i(t'')]]^2}{2\bar{d}_i} + L_i + X_i^{\text{safe}} \tag{29}$$

where $v_{j_\ell+1}(t'')$ represents the instantaneous speed of the rear vehicle $j_\ell+1$ at time t''; $\tau_{j_\ell+1}$ refers to the driver's reaction time associated with the rear vehicle $j_\ell+1$; $\bar{d}_i$ and $\bar{d}_{j_\ell+1}$ represent the expected decelerations associated with the target vehicle i and the rear vehicle $j_\ell + 1$ in response to any potential emergency conditions present ahead, and both of them are negative values.

- Condition 4: Restriction of the dynamic safety spacing between the target vehicle i and the new front vehicle j_ℓ in the adjacent lane (ℓ).

This condition serves to deal with the constraint of the dynamic safety spacing between the target vehicle i and the front vehicle j_ℓ present in the adjacent lane (ℓ) in the process of the target vehicle's lane changing. Similarly, based on the aforementioned concept, the following condition Eq. (30) must hold to ensure that the lane-changing maneuver of the target vehicle can be safely completed at time $t'' + \Delta t_i$.

$$x_i(t'' + \Delta t_i) - X^c_{i \to j_\ell}(t'' + \Delta t_i) \geqslant 0$$

$$\Rightarrow x_i(t'') - \left\{ v_i(t'') \times \tau_i - \frac{[v_i(t'')]^2}{2\bar{d}_i} \right\}$$

$$- \left\{ x_{j_\ell}(t'') + \frac{[v_{j_\ell}(t'')]^2}{2\bar{d}_{j_\ell}} + L_{j_\ell} + X_i^{\text{safe}} \right\} \geqslant 0$$

$$\Rightarrow x_i(t'') - x_{j_\ell}(t'') \geqslant \left\{ v_i(t'') \times \tau_i - \frac{[v_i(t'')]^2}{2\bar{d}_i} \right\}$$

$$+ \frac{[v_{j_\ell}(t'')]^2}{2\bar{d}_{j_\ell}} + L_{j_\ell} + X_i^{\text{safe}} \qquad (30)$$

where $X^c_{i \to j_\ell}$ represents the potential conflict point between the target vehicle i and the front vehicle moving ahead in the corresponding adjacent lane (ℓ); $x_{j_\ell}(t'')$ and $v_{j_\ell}(t'')$ represent the instantaneous location and speed of the front vehicle j_ℓ present in the adjacent lane (ℓ) at time t''; $\bar{d}_{j_\ell}$ represents the deceleration of the front vehicle j_ℓ expected by the target driver i in the corresponding lane-changing process; L_{j_ℓ} represents the physical length of the front vehicle j_ℓ.

3. Numerical results

This section describes the major procedures of experimental design and the resulting numerical results to demonstrate the feasibility of the proposed methodology in characterizing incident-induced dynamic driving behavior. Considering the intricate nature of incident-induced driving behavior and difficulties in the corresponding data acquisition, the current effort devoted in this scenario mainly aims at calibrating and validating the proposed model in the car-following aspect. The main techniques utilized for performance evaluation include the Paramics microscopic traffic simulator and a specific microscopic traffic simulation program, which was coded with the Turbo C++ computer language, developed particularly for this study. Herein, the proposed incident-induced intra-lane traffic model including the quantum mechanics-based glancing-around and rubbernecking-driven car-following models were embedded into the developed traffic simulation program. Evaluation measures were based mainly on comparison of
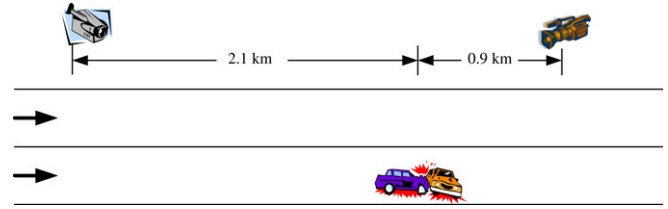

Fig. 5. Scheme of the study site.

the simulation data generated from the developed traffic simulation program with both video-based real incident data and simulation data output from Paramics, which is a well-known microscopic traffic simulator.

The procedure of data acquisition adopted in this study, involves two scenarios: (1) video-based data processing for model calibration and testing, and (2) simulation data generation for model validation.

The database generated in the first scenario was primarily processed from the video-based data, which were collected with the aid of Taiwan Area National Freeway Bureau (TANFB). The study site was aimed at 3-km 2-lane mainline segment of the northbound N-1 freeway in Taiwan, where two probe vehicles were artificially placed across the shoulder and outside lane of the study site to mimic a rear-end collision event, as illustrated in Fig. 5. Two cameras were installed, respectively, at the upstream and downstream sections of the incident site to videotape the lane traffic movements for fifteen minutes during the incident period. Based on the videotapes, Traffic data including lane traffic arrival rates, densities, approaching speeds, flows, and the corresponding arrival and departure times of these sampled vehicles were generated.

The generated video-based data were then used to calibrate the parameters of the Paramics microscopic traffic simulator. The primary input data and the calibrated parameters set used for simulation are summarized in Table 1. Here, certain key parameters, e.g., the physical size, the average reaction time, the maximum acceleration and deceleration rates, and the minimum allowable vehicular headway embedded in Paramics were specified. In addition, we also examined the distributions in terms of the arrival rate and the arrival speed, yielding the related test results presented in Table 1.

In the second scenario, the Paramics microscopic traffic simulator was utilized for the calibration and validation of the proposed model. Based on the processed video-based data, a simulation network mimicking the study site was constructed using Paramics. Furthermore, the function of vehicular dashboard tracer embedded in Paramics was actuated. Here, using such a function, a Paramics user is allowed to trace any given simulated vehicle, and manipulate the traced vehicle with lane changing as well as acceleration and deceleration maneuvers during simulation, mimicking the mechanisms of a driving simulator.

To calibrate the key parameters of the proposed model, we randomly drew 52 samples as volunteers with driver licenses from the staff and graduate students of a university in northern Taiwan. In each simulation event, simulated vehicles were set to run in real time, where one of the simulated vehicles

Table 1
Summary of the static characteristics of vehicles and calibrated traffic parameters

Vehicle type		Length (m)	Width (m)	Top speed (km/h)	Composition (%)	Max. acceleration (m/s^2)	Max deceleration (m/s^2)
Light vehicle	Car	4.0	1.6	158.4	78	3.56	7.30
	Light goods vehicle (lgv.)	6.0	2.3	126.0	14	2.22	7.30
Heavy vehicle	Truck	11.0	2.5	118.8	5	1.4	5.63
	Bus	10.0	2.5	61.2	3	1.4	5.63

Testing with respect to the arrival rate (assumed to follow a negative binomial distribution)

Samples	Mean value (veh/10 s)	Standard deviation (veh/10 s)	Chi-square estimate	Critical value	Result
316	3.58	1.19	9.74	11.07	Accepted

Testing with respect to the arrival speed (assumed to follow a normal distribution)

Type of vehicle	Sample	Mean value (m/s)	Standard deviation (m/s)	P-value	Level of significance	Result
Car	185	27.4	2.77	4.92	0.1	Accepted
Lgv.	59	26.6	2.26	2.55	0.1	Accepted
Truck	33	24.9	1.84	0.29	0.1	Accepted
Bus	39	25.1	1.93	0.57	0.1	Accepted

Other key parameters

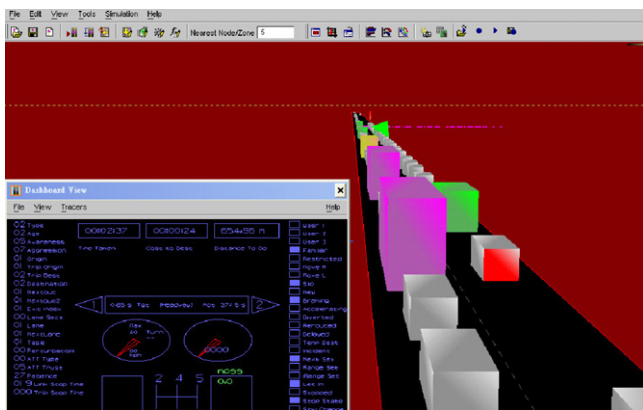| The average reaction time (s)	The minimum acceptable headway (s)
0.78	0.85

Fig. 6. Illustration of the simulated-vehicle manipulation function.

Fig. 7. Framework of the proposed microscopic traffic simulation program.

present in the adjacent lane was randomly selected to trace as it entered into the simulated study site. Meanwhile, one sampled volunteer was asked to manipulate the given traced vehicle at will via the aforementioned dashboard tracer function, as illustrated in Fig. 6, to pass by the simulated incident. The corresponding traffic characteristics, including the types and locations of the traced vehicle and the corresponding surrounding vehicles as well as their instantaneous speeds and accelerations/decelerations were collected to calibrate the parameter, including h, α_1, α_2, and α_3, particularly embedded in the quantum mechanics-based glancing-around and rubbernecking-driven car-following models.

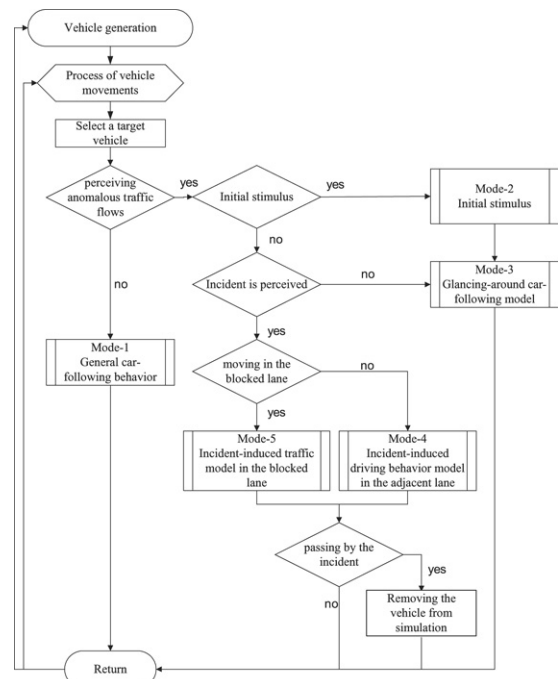Utilizing the calibrated parameters and models proposed, a specific microscopic traffic simulation program was developed in the Turbo C++ computer language. The framework of the proposed simulation program is shown in Fig. 7, involving five major subroutines (termed mode-1 to mode-5), where mode-2 to mode-4 embed the proposed models particularly to deal with the vehicles approaching the incident site via the adjacent lane.

Table 2
Summary of the comparison results (arrival volume)

| Data source | Sampling interval | | | | | |
| | Aggregate arrival volume (veh/5 min) | | | Aggregate arrival volume (veh/15 min) | | |
	Light vehicle	Heavy vehicle	Total	Light vehicle	Heavy vehicle	Total
Video-based data	164	51	215	498	148	646
Proposed model	159	49	208	479	156	635
Paramics	157	45	202	471	139	610
Relative error associated with the proposed model (%)	−3.0	−3.9	−3.3	−3.8	5.4	−1.7
Relative error associated with Paramics (%)	−4.3	−11.8	−6.0	−5.4	−6.1	−5.6

Table 3
Summary of the comparison results (departure volume)

| Data source | Sampling interval | | | | | |
| | Aggregate arrival volume (veh/5 min) | | | Aggregate arrival volume (veh/15 min) | | |
	Light vehicle	Heavy vehicle	Total	Light vehicle	Heavy vehicle	Total
Video-based data	125	39	164	378	115	493
Proposed model	117	40	157	365	110	475
Paramics	110	32	142	329	99	428
Relative error associated with the proposed model (%)	−6.4	2.6	−4.3	−6.1	−4.3	−3.7
Relative error associated with Paramics (%)	−12.0	−17.9	−13.4	−13.0	−13.9	−13.2

Table 4
Summary of the comparison results (average link travel time)

| Data source | Criteria | |
	Average link travel time (s)	Relative error (%)
Video-based data	125.4	
Proposed model	118.2	−5.7%
Paramics	149.3	19.1%

In contrast with mode-4, mode-5 aims at the vehicles moving in the blocked lane upstream to the incident site, embedding the respective lane traffic models developed previously. The details about the model formulation and evaluation can be found elsewhere [27]. Note that the focus of this scenario is on verifying the validity of the proposed incident-induced adjacent-lane traffic behavior models using the developed simulation tool. Also, calibration of the proposed traffic simulation tool is needed, which was conducted previously to the model tests.

To evaluate the proposed models, we compared the simulation data generated from the proposed incident-induced traffic simulation program with both the video-based real incident data and the Paramics simulation data in the following test scenario. Herein, four types of traffic measures are utilized, including: (1) the aggregate arrival volume, (2) the aggregate departure volume, (3) the average link travel time, and (4) the lane usage. Herein, both the arrival and departure volumes were used to test the acceptability of the simulated lane traffic flows entering into and exiting from the study site; in contrast, the average link travel time and lane usage were used to evaluate the system performance of the proposed models in characterizing the incident-induced lane traffic maneuvers. The comparison results are summarized in Tables 2–6, where all the simulated values shown in this table were the aggregated measurements via 10-run simulations for each event. A discussion on comparison results is provided in the following.

Overall, the numerical results shown in the above tables may reveal the validity of the proposed approach in characterizing the incident-induced driving behavior. Here, all the estimated errors of the proposed method relative to the video-based data fall within the range of −10% and 10%. In addition, several generalizations are further provided for explication.

(1) Given the same traffic arrival patterns, the resulting traffic flows leaving the incident site yielded from the proposed model may fit in with the corresponding video-based data, compared to the simulated data obtained from Paramics. Relative to the video-based data, both proposed model and Paramics may be able to capture the traffic arrival patterns to a certain extent; however, the proposed model appears to outperform Paramics in characterizing the incident-induced driving behavior, thus resulting in a relatively lower estimation error in either 5 min or 15 min data sampling cases.

(2) In the aspect of the average link travel time, the result of the proposed model may remain valid since the simulation error relative to the video-based data is −5.7%, which is significantly lower than that of Paramcis (i.e., 19.1%). This may imply the significance of respective incident-induced driving behavior models in improving incident traffic characterization and simulation.

(3) The simulated lane traffic distribution and the resulting traffic densities generated by the proposed model are greatly acceptable, compared to the output from Paramics. According to our observations from simulations, such a generalization should also rely, to a certain extent, on the integration of the proposed models with the respective incident-induced lane-changing model embedded in model-5, which was previously developed to deal particularly with the incident-induced traffic behavior in blocked lanes. Therefore, the resulting multi-lane traffic usage yielded from the proposed method is almost consistent with the video-based data.

Table 5
Summary of the comparison results (lane usage)

Data source	Criteria			
	Lane usage (%)		Relative error (%)	
	Adjacent lane	Blocked lane	Adjacent lane	Blocked lane
Video-based data	68.3	31.7		
Proposed model	66.5	33.5	2.6	5.7
Paramics	56.6	43.4	17.3	36.9

Table 6
Test results of simulated headway distributions

Simulated data group	Collection location upstream from the incident site (km)	Chi-square value	Critical point with significance level $\alpha = 0.1$	Degrees of freedom	Test result
1	2.4	5.7	10.64	6	Accepted
2	2.1	4.2	10.64	6	Accepted
3	1.9	6.5	10.64	6	Accepted
4	1.5	7.9	10.64	6	Accepted
5	1.3	8.9	10.64	6	Accepted
6	1.0	8.6	10.64	6	Accepted
7	0.6	9.7	10.64	6	Accepted
8	0.4	10.4	10.64	6	Accepted
9	0.1	23.1	10.64	6	Not accepted
10	0.0	8.2	10.64	6	Accepted

Furthermore, the potential advantages of the proposed models with respect to depicting incident-induced lane traffic behavior have also been revealed in comparison with the Paramics microscopic traffic simulator. This generalization may support our claim, in this paper, on the urgent need of developing respective driving behavior models to characterize the incident-induced lane traffic phenomena.

Despite the acceptability of the proposed model's capability, demonstrated above, in macroscopic traffic flow characterization, the model's potential in reproducing the reality of the corresponding microscopic traffic behavior should also need to be examined. For this reason, the consistency of the inter-vehicle headway distributions generated by the proposed model and the video-based data was examined as follows.

First, the inter-vehicle headways measured at certain locations of the study site were collected from the video-based data, where ten locations upstream from the incident site were randomly selected to measure the corresponding headways of vehicles moving in adjacent lanes. Assuming that the collected ten groups of video-based headway measurements follow respective Pearson Type-III distributions, according to the previous literature [19], we tested if the simulated data yielded from the proposed model follow a consistent distribution for each sampling location. Here, the primary procedures for testing the hypothesis are presented in Fig. 8, and considering the space limit, these procedures as well as the corresponding interim output data are not presented in this paper. Through 10-run simulations, which are the same as the above test scenario, the final test results of the simulated data groups are summarized in Table 6.

As can be seen in Table 6, the test results of simulated headway distributions are overall accepted expect for the data group 9, which is located 0.2 km upstream from the incident
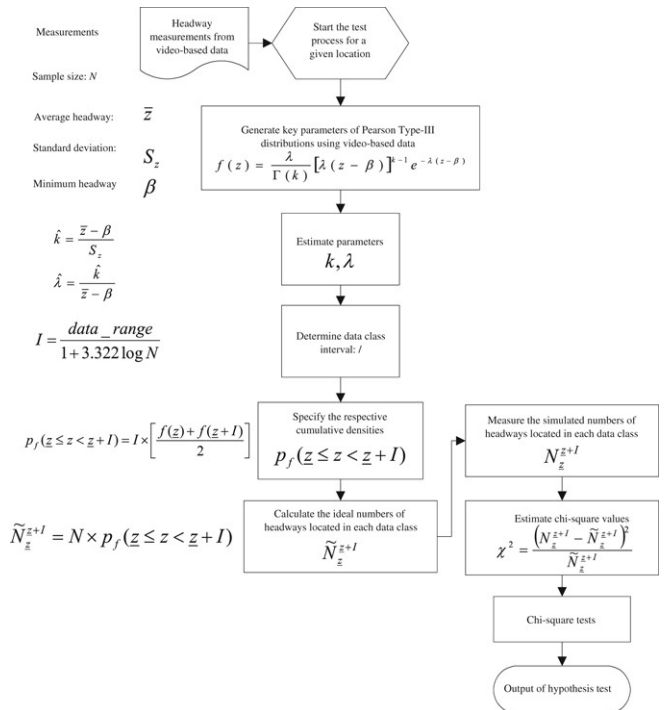

Fig. 8. Primary procedures for examining simulated headway distributions.

site. Several important findings from the tests are provided in the following.

First, the corresponding lower values of the chi-square statistics shown in this table imply that the headway patterns measured beyond 1.5 km upstream from the incident site were captured pretty well using the proposed quantum mechanics-based glancing-around car-following model. It is also induced that the glancing-around car-following behavior reproduced by

the proposed model appears to exist upstream from the incident site before the occurrence of drivers' perception of the incident.

Second, due to the increase in the incident-induced lane-changing effects from the blocked lane, the headway patterns of the adjacent lane may turn out to be more anomalous as collected towards the incident site. Such an argument may be true particularly as the continuity of intra-lane traffic flow is significantly and frequently disturbed by the lane-changing vehicles from the blocked lane, as revealed by the chi-square statistics associated with data groups 7, 8, and 9, which were collected within 1.0 km upstream from the incident site.

Third, despite the fact that the test result associated with data group 9 is not acceptable, there is no strong reason for denying the validity of the proposed model in characterizing the incident-induced rubbernecking-driven car-following behavior. According to our observation from the videotape, it was found that a certain number of lane-changing vehicles from the blocked lane appeared to significantly interrupt the continuity of the adjacent-lane traffic flow near the incident site, thus contributing to the unexpected variations of headways exhibited in data group 9. Correspondingly, the headways measured at the adjacent lane near the incident site may no longer be fully composed of the pairs of remaining vehicles moving in the adjacent lane; under certain conditions, they may be composed of the mixed traffic flow or the vehicles unexpectedly conducting lane changing from the blocked to the adjacent lane very close to the incident site. This is why we still accept the overall performance of the proposed model in characterizing the incident-induced lane traffic behavior near the incident site.

Fourth, compared to data group 9, the headways exhibited in data group 10 appear to be relatively consistent with those measured from video-based data. It is worth mentioning that the measurements of data group 10 were collected just at the location right adjoining to the incident event, where the corresponding lane-changing effect might not be as significant as what happened upstream from the incident site. In the test scenario (i.e., a medium-volume incident case), it was observed that most of the drivers present in the blocked lane appeared to be able to complete lane-changing maneuvers before reaching the incident site. Thus, the resulting lane-changing effect on data group 10 turned out to be less significant than that on data group 9, leading to such a generalization.

Despite the above test results, which may help to prove the feasibility of the proposed model in characterizing microscopic traffic maneuvers, several limitations of this study are summarized in the following for future consideration.

(1) The queuing and lane-changing effects oriented from the blocked lane may remain as significant factors influencing the drivers' behavior of the adjacent lane while they are approaching to the incident site. Furthermore, such effects may also vary with time and space, as well as the instantaneous traffic flow conditions, as illustrated in the previous literature [30,29]. However, testing the proposed model under diverse lane-changing and queuing scenarios has not yet been taken into account in the present experimental design.

(2) The present study case is limited to the lane blockage in a two-lane mainline freeway segment such that the proposed model serving to deal with incident-induced lane-changing maneuvers from the adjacent lane to the other farther adjacent lanes has not been tested.

(3) Due to the limitations of advanced instruments in collecting enough real incident data and the potential drivers' responses to the resulting incident-induced traffic flows, the prototype of the proposed quantum mechanics-based approach to incident-induced driving behavior may not be effectively calibrated and tested in the present preliminary tests.

4. Conclusions and recommendations

This paper has presented a quantum mechanics-based approach to modeling the dynamic driving behavior in the process of passing by a lane-blocking incident via the adjacent lane. Considering the potential effects of drivers' psychological factors on the aforementioned incident-induced driving behavior, a quantum mechanics-based methodology is proposed by incorporating several psychological factors, including the stimulus arising from the variations of optical flows, curiosity, and internal pressure into the model formulation. Then, a microscopic traffic behavior module, which consists of three sequential phases, including (1) initial stimulus, (2) glancing-around car-following, and (3) incident-induced driving behavior, is formulated for characterizing the dynamic driver behavior in the entire process of passing by an incident site, followed by the development of a microscopic simulation model to test the validity of the proposed method.

Our preliminary test results have implied that the proposed microscopic driver behavior models permit reproducing the dynamics of incident-induced driving behavior using quantum mechanics-based methodology. Particularly, it appears feasible to reformulate the corresponding car-following models based on the concepts of quantum mechanics-based optic flow variations, as claimed in [1]. Moreover, the proposed method exhibited its potential advantages for the application of analyzing microscopic traffic maneuvers under the conditions of freeway lane-blocking incidents in comparison with the existing microscopic traffic simulators.

Nevertheless, more elaborate experimental design involving the utilization of advanced devices for data collection and model testing is apparently needed. For instance, we are presently testing the model under various traffic flow scenarios, where a variety of traffic arrivals as well as the effects of lane-changing and queuing effects of the blocked lane is considered. Furthermore, we attempt to further test the proposed methodology in a multi-lane mainline segment such that the embedded incident-induced lane-changing model can also be examined. In addition, elaborate examinations of the postulated assumptions may be needed in future research. The applications of the quantum mechanics-based approach to the formulation of dynamic driving behavior may also warrant more research. These include the use of the proposed

J.-B. Sheu / Physica D 237 (2008) 1800–1814

approach in reproducing incident-free car-following and lane-changing maneuvers on either freeways or surface streets. More importantly, it is expected that this study can not only provide the feasible access to a better understanding of the influence of human psychological and physical factors in driving behavior to improve road safety, but also stimulate more researchers devoted to exploring more related issues and solutions to add more value to the literature of applied physics and related areas.

Acknowledgment

References

[1] R.G.V. Baker, On the quantum mechanics of optic flow and its application to driving in uncertain environments, Transp. Res. F 2 (1999) 27–53.
[2] R.G.V. Baker, On the kinematics and quantum dynamics of traffic flow, Trans. Res. B 17 (1983) 55–66.
[3] R.G.V. Baker, A model of traffic dispersion from a congested road, Trans. Res. B 15 (1981) 319–327.
[4] D. Bartmann, W. Spijkers, M. Hess, Street environment, driving speed and field of version, in: A.G. Gale, I.D. Brown, C.M. Haslegrave, I. Moorhead, S.P. Taylor (Eds.), Version in Vehicles III, Elsevier, Amsterdam, 1991.
[5] A. Beiser, Perspectives of Modern Physics, McGraw-Hill, New York, 1969.
[6] M. Brackstone, M. McDonald, Car-following: a historical review, Transp. Res. F 2 (1999) 181–196.
[7] V. Cavallo, M. Laurent, Visual information and skill level in time-to-collision estimation, Perception 17 (1988) 623–632.
[8] P. Chakroborty, S. Kikuchi, Evaluation of the general motors based car-following models and a proposed fuzzy inference model, Transp. Res. C 7C (4) (1999) 209–235.
[9] Y.-H. Chou, J.-B. Sheu, A simulation model of mixed traffic flow in roundabouts, Transp. Planning J. 21 (3) (1992) 301–333.
[10] C.F. Daganzo, J.A. Laval, Moving bottlenecks: a numerical method that converges in flows, Transp. Res. B 39 (9) (2005) 855–863.
[11] J.A. Fodor, The Modularity of Mind, The MIT Press, Cambridge, MA, 1983.
[12] J.J. Gibson, The Senses Considered as a Perceptual System, Houghton Mifflin, Boston, 1966.
[13] R.W. Hall, Incident dispatching, clearance and delay, Transp. Res. A 36 (1) (2002) 1–16.
[14] E.N. Holland, A generalized stability criterion for motorway traffic, Transp. Res. B 32 (2) (1998) 141–154.
[15] H.J. Kayser, M. Hess, The dependency of drivers' viewing behavior on speed and street environment structure, in: A.G. Gale, I.D. Brown, C.M. Haslegrave, I. Moorhead, S.P. Taylor (Eds.), Version in Vehicles III, Elsevier, Amsterdam, 1991.
[16] S. Kikuchi, P. Chakroborty, Car-following model based on fuzzy inference system, Transp. Res. Record 1365 (1992) 82–91.
[17] D.N. Lee, The optic flow field: the foundation of vision, Philos. Trans. R. Soc. 290 (1980) 169–179.
[18] R.W. MacLeod, H.E. Ross, Optic flow and cognitive factors in time-to-collision estimates, Perception 12 (1983) 417–423.
[19] A.D. May, Traffic Flow Fundamentals, Prentice Hall, Englewood Cliffs, NJ, 1990.
[20] C.J. Messer, C.L. Dudek, J.D. Friebele, Method for predicting travel time and other operational measures in real-time during freeway incident conditions, Highway Res. Record 461 (1973) 1–16.
[21] M.A. Mossison, Understanding Quantum Physics: A User Manual, Prentice-Hall, New Jersey, 1990.
[22] T. Miura, Behavior oriented version: functional field of view and processing resources, in: J.K. O'Regan, A. Levy-Schoen (Eds.), Eye Movements: From Physiology to Cognition, Elsevier, Amsterdam, 1987.
[23] G.F. Newell, Flows upstream of a highway bottleneck, in: A. Ceder (Ed.), Transportation and Traffic Theory, Pergamon, Amsterdam, NL, 1999, pp. 125–146.
[24] G.F. Newell, A simplified theory of kinematic waves in highway traffic, part II: queuing at freeway bottlenecks, Transp. Res. B 27B (4) (1993) 289–303.
[25] N. Osaka, Speed estimation through restricted visual field, in: A.G. Gale, M.H. Freeman, C.M. Haslegrave, P. Smith, S.P. Taylor (Eds.), Version in Vehicles II, Elsevier, Amsterdam, 1988.
[26] T.A. Ranney, Psychological factors that influence car-following and car-following model development, Transp. Res. F 2 (1999) 213–219.
[27] J.-B. Sheu, A composite traffic flow modeling approach for incident-responsive network traffic assignment, Physica A 367 (2006) 461–478.
[28] J.-B. Sheu, Y.-H. Chou, A. Chen, Stochastic modeling and real-time prediction of incident effects on surface street traffic congestion, Appl. Math. Modelling 28 (5) (2004) 445–468.
[29] J.-B. Sheu, A stochastic modeling approach to real-time prediction of queue overflows, Transp. Sci. 37 (1) (2003) 97–119.
[30] J.-B. Sheu, Y.-H. Chou, L.-J. Shen, A stochastic estimation approach to real-time prediction of incident effects on freeway traffic congestion, Transp. Res. B 35B (6) (2001) 575–592.
[31] J.-B. Sheu, S.G. Ritchie, Stochastic modeling and real-time prediction of vehicular lane-changing behavior, Transp. Res. B 35B (7) (2001) 695–716.
[32] H.M. Zhang, T. Kim, A car-following theory for multiphase vehicular traffic flow, Transp. Res. B 39 (5) (2005) 385–399.